Overview of the Mineral-PET run-of-mine Diamond bearing rock sorter

M Cook[1], M Tchonang[1], E Chinaka[2], M Bhamjee[1], F Bornman[3], SH Connell[1]

[1] University of Johannesburg, Johannesburg, South Africa
[2] Necsa, South Africa
[3] Multotec, Johannesburg, South Africa

E-mail: shconnell@uj.ac.za

Abstract. Mineral-PET is a technology for the sorting of diamond bearing rock (kimberlite ore) based on a mineral analogue of the well-known medical Positron Emission Tomography (PET) imaging technique. The naturally occurring carbon in kimberlite needs to be activated via photonuclear transmutation before it can be imaged. For the R&D phase of the project, a technology demonstrator has been built. This is a planar PET array built around a conveyor belt using kimberlite phantoms. The phantoms consist of blocks of cement with the radioactive material (^{22}Na) uniformly distributed throughout it to simulate the homogenous background radiation from various non-diamond PET emitters. Diamonds are modeled in the phantom by the inclusion of a localized hot-spot of ^{22}Na. This system has been used to benchmark computational simulations and to explore the physics issues for the specification of a pilot scale plant at a mine. The review will provide new results and updates on the performance and outlook for Mineral-PET.

1. Introduction

The detection and imaging of diamonds within coarse crushed kimberlite rocks can be carried out in a run-of-mine scenario. This promises large savings and reduced diamond breakage. A schematic showing the Mineral-PET process is shown in figure 1. The device is inserted into the kimberlite processing chain after the coarse crush, which breaks rocks up into roughly 10 cm pieces. The stream is then sent to an irradiation hopper where an electron beam incident on a tungsten target creates gamma rays via bremsstrahlung. The beam is fanned out over a 1 m^2 area via perpendicularly oriented bending magnets. The gamma rays are incident on the kimberlite, which is several layers deep to maximise usage of the gamma beam. The gamma rays convert ^{12}C in diamonds and within the surrounding material to the radioactive PET isotope ^{11}C, making use of the giant dipole resonance in the ^{12}C$(\gamma, n)^{11}$C cross section. The rock is then stored for about 20 minutes in a hold hopper to allow the non-carbon background signal to die away. After the decay period, the kimberlite is directed onto a conveyor belt and the rocks then pass between two horizontally oriented planar PET detector arrays. Each node of a cluster computer is assigned a volume of space between the detectors in a revolving fashion. As coincident events are detected, corresponding trajectories are reconstructed, and images gradually built up in the volumes traversed by each trajectory. When the volume reaches the end of the detection region, the relevant node then analyses the 3D PET image, and decides

whether or not a diamond is present. This information is fed to an ejection system, which separates diamond bearing rock, allowing the remainder to be discarded.
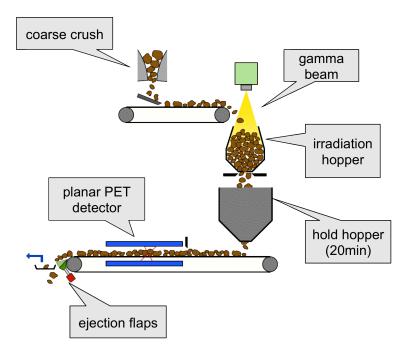

Figure 1. Run-of-mine Mineral-PET schematic [1].

Simulations and calculations have been made to optimise imaging algorithms, determine the expected activity levels and to optimise electron beam parameters and detector layout. Results show that a 5mA, 40MeV accelerator and a 2 m^2 bi-planar PET array could reliably detect diamonds smaller than 1 mm at a kimberlite throughput of 700 tonnes/hour, assuming 0.054% homogeneously distributed non-diamond carbon. Larger diamonds are more easily detected, with the detection probability growing faster than the diamond volume. An analysis of data taken at a 100 MeV electron accelerator shows that all non-PET activations are of a similar order of magnitude to the natural background activity. All the radiological implications reduce to below IAEA guidelines within two hours, and the material is radiologically equivalent to natural background within 2 days. A scaled down version of the Mineral-PET system has been constructed as a technology demonstrator, where the detector system has a reduced size and the activation system is represented by phantoms. It successfully identifies simulant diamonds within these phantoms and validates the simulations. The resolution is optimised by a custom genetic algorithm which adjusts various detector parameters in a hierarchical manner. Two complimentary techniques to determine radiological exposure are developed, which indicate that the exposure levels at Mineral-PET will be easily manageable. These aspects are all described in more detail in this reference [2].
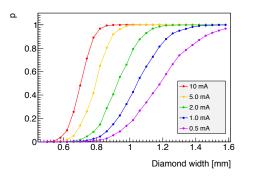
2. Simulation of Activation and Minimum Detection Limits
The activation stage of the Mineral-PET has been simulated with GEANT4. One set of simulations studied the power efficiency of different electron accelerator energies, beam currents, converter materials and thicknesses. The power efficiency is defined as the number of useful gamma rays created per incoming electron, divided by the beam energy. Useful gamma rays are gamma rays likely to excite the giant dipole resonance of carbon ($^{12}C(\gamma, n)^{11}C$), taken as between 20MeV and 27MeV. The power efficiency plateaus after about 40MeV, so this is chosen

as the Mineral-PET beam energy. Gold and tungsten bremsstrahlung targets perform equally well, so a 3 mm tungsten target is chosen due to its superior strength and high melting point.

The mixed radiation field arising from both this accelerator-converter configuration and for the subsequent penetration into a total depth of kimberlite of 30cm was also modelled using GEANT4. This depth of kimberlite corresponds to about three radiation lengths, and can therefore be taken as the effective activation depth for the Mineral-PET process. The results of this calculation were used to determine the production of both the ^{11}C and ^{15}O PET isotopes. The dominant background for Mineral PET a few minutes after irradiation is the activity from ^{15}O as there are many oxides in the kimberlite ore. This component is no longer dominant after the residence period in the hold hopper. The ^{11}C activity arises from either the presence of a diamond or from the very dilute presence of homogenously distributed carbon (carbon dioxide and carbonates). The Mineral-PET detector system was also modelled by Monte Carlo to determine the overall detection efficiency. This calculation could also be used to optimise the planar detection geometry. A study was performed of overall Mineral-PET resolution for the reconstruction of hot spots of ^{11}C PET activity. This includes the detector position resolution, and the effective positron range and non-colinearity smearing. A novel hybrid diamond detection algorithm was developed which will be discussed elsewhere. Ultimately, a diamond is identified when the number of trajectories (the Line of Response (LoR) formed by the back-to-back decay photons) that intersect a region of interest (ROI) passes a given threshold. The threshold is dependent on the tolerated false positive rate, the size of the diamond to be detected, the resolution of the detection system, the level of ^{11}C activation and the amount of homogenously distributed non-diamond carbon in the kimberlite. Combining the results of an analytic formulation of the physics of the diamond detection with a Monte Carlo procedure to determine the parameters in the model, the diamond detection probability could be evaluated.

Figure 2 shows the simulated probability of detecting a diamond as a function of diamond length, for various different beam currents. Mineral-PET should have a 99.7% chance of finding a 1mm diamond with a beam current of 5mA when the non-diamond carbon concentration is below 0.2% CO_2.
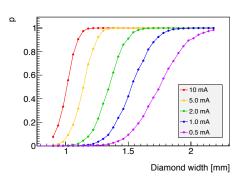

Figure 2. Probability to find diamonds in a 0.2% CO_2 (left) and a 2% CO_2 (right) background as a function of diamond size, for various beam currents.

3. Residual Activity Identification, Monte Carlo Validation
A sample of kimberlite irradiated at the Aarhus University microtron ($E_e = 100$ keV) is shown in figure 3. This is a two dimensional histogram, with elapsed time on one axis and energy on the other. The PET line at 511 keV is far larger than other sources of activity. The change of

slope of this line as the oxygen signal decays and the carbon signal starts to dominate is evident. Most other species quickly decay. The peak at just under 1500 keV is the potassium-40 peak.
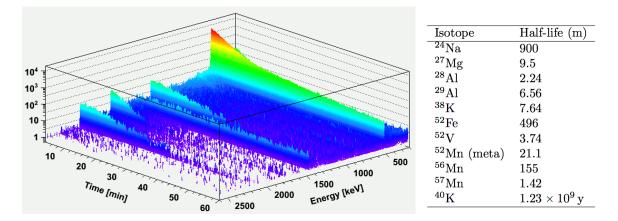

Isotope	Half-life (m)
^{24}Na	900
^{27}Mg	9.5
^{28}Al	2.24
^{29}Al	6.56
^{38}K	7.64
^{52}Fe	496
^{52}V	3.74
^{52}Mn (meta)	21.1
^{56}Mn	155
^{57}Mn	1.42
^{40}K	1.23×10^9 y

Figure 3. Left : Two dimensional energy - elapsed time spectrum of photon irradiated kimberlite showing induced PET activity and the activation of various isotopes. Right : The identification of isotopes responsible for the residual activity in using both peak energy and lifetime. [1].

The first goal was to comprehensively understand all the isotopes that are excited during irradiation. The second goal was to obtain well calibrated experimental data on the activation process for comparison to simulations including the detailed mixed radiation field at two different energy distributions. The first goal has been achieved, as the combined information of peak energy and lifetime enable a unique identification of the various isotopes which have been activated. Of these isotopes, the long-lived ones are ^{24}Na, ^{52}Fe, ^{56}Mn and ^{40}K. The potassium can be discounted, because it is present at roughly the same level in non-irradiated samples. The observed initial activities for 1 cc of kimberlite from the irradiation (about 60 times the dose envisaged for the Mineral-PET method) are: for ^{56}Mn : 1.41 ± 0.04 Bq, for ^{24}Na : 2.81 ± 0.02 Bq. The fact that the size of the naturally occurring potassium is comparable to that of the isotopes that have been activated is indicative of the fact that very little radiation has been induced. The ^{24}Na could be a concern, as it is easily metabolised. However, all the radiological implications reduce to below IAEA guidelines within two hours, and the material is radiologically equivalent to natural background within 2 days. The Mineral-PET method can therefore be considered radiologically safe.

With respect to the second goal, the GEANT4 simulation was used to model the mixed radiation field and from there the activation could be calculated. The simulation results were within a factor of 2 and 3 for the carbon and oxygen and 5 for the sodium with respect to the experimental results. The modelling of the residual activity is therefore partially successful, and the remaining disagreement is attributed to possible variations in the kimberlite composition, as well as uncertainties in the irradiated dose estimation.

4. Technology demonstrator
A scaled down version of the full Mineral-PET detector system built around a conveyor belt has been created as a laboratory demonstrator. This serves as a proof of concept, and allows experimentation with detector technology, detector alignment optimisation, software development etc. An accelerator has not yet been secured, so results using the laboratory demonstrator have been acquired using ^{22}Na sources, which have been incorporated into kimberlite, in such a way as to emulate the activity profile of photon irradiated kimberlite,

with and without incorporated diamonds. The technology demonstrator is able to locate a diamond simulant in the background of homogenously distributed carbon simulant within a kimberlite phantom moving on a conveyor belt through the Mineral-PET detector array. The visualisation of the detection is evidenced by a digital presentation of the lines of response (LoR) recorded by the detectors in real time, and the painting of the location of the diamond on the kimberlite phantom by a data projector. The quantitative results are consistent with the simulations discussed above.

5. Radiological Exposure Modelling

One of the concerns for an industrial scale Mineral-PET plant is the radiation exposure of workers. The shielding requirements for the irradiation system have already been investigated in [3]. This included radiation shielding calculations, analysis, and optimisation with the aid of the MCNPX Monte Carlo code. The conclusion was that a 1.6 m thick shielding matrix of lead, iron, wax and boron carbide adequately shielded personnel from the irradiation system. If the accelerator, irradiation system and hold hopper were buried underground away from personnel, these requirements would be less stringent.
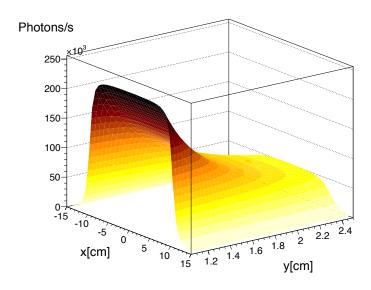
Once the kimberlite is out of the hold hopper, we would like to quantify the exposure received by Mineral-PET workers in common scenarios, for example nearby the conveyor belt or a pile of mine tailings. Two numerical techniques have been developed to calculate the exposure given a particular geometry of radioactive material. The first uses an attenuation model to arrive at an integral that can be solved numerically. This technique only applies to cuboid shaped bodies of material. The results of this are compared to a full Monte Carlo physics simulation that is more accurate, but far more computationally intensive. The second technique can, however, be applied to any geometry. The development of the radiological assessment tools have already been presented in [4].
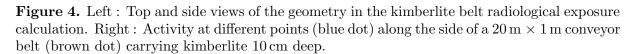
Here we present additional results specifically for the case that will occur in a Mineral-PET plant. This is of a body of kimberlite 10 cm deep on a 1 m wide conveyor belt, after irradiation has occurred and the decay time has passed. Figure 4 shows the geometry, consisting of a 20 m long kimberlite stream, 1 m wide and 10 cm tall. The 50 cm radius water ball is shown one metre away from the kimberlite at a height of 30 cm. We will use the 0.2% carbon dioxide activity estimate, and assume that 29 minutes have passed since irradiation. At this time, the carbon and oxygen signals dominate, so we ignore the contribution from sodium. The combined specific activity of the carbon and oxygen is $33.9 \, \text{Bq/cm}^3$. Each decay creates two 511 keV photons, so the overall 511 keV gamma rate is 67.8 Hz/g.

Figure 4 on the right shows the activity absorbed by the target as a function of the position of the centre of the target. The conveyor belt extends from $x = -10 \, \text{m}$ to $x = 10 \, \text{m}$, and from $y = -0.5 \, \text{m}$ to $x = 0.5 \, \text{m}$. The edge of the target is 5 cm from the belt at its closest, and the centre of the target is 30 cm above the belt. This approximates a worker standing at various positions next to the conveyor belt. Both the activity in Bq/cm^3 and the gamma attenuation constant are multiplied by 0.7 to take the packing density into account.

The activity that hits the target when it is 5 cm from the middle of the belt is 2.40×10^5 photons/s. Considering a photon energy of 511 keV and a gamma radiation quality factor of 1 [5], this corresponds to $70.8 \, \mu\text{Sv/h}$. At a distance of 1 m, this has already fallen to 7.50×10^4 photons/s or $22.1 \, \mu\text{Sv/h}$. Workers would have to spend six hours a day for 118 days at a distance of 5 cm, to reach the 50 mSv level set in the IAEA safety guide relating to radioactive material in mining [6]. Workers could be employed full time at a distance of 1 m.

Note that the kimberlite will be more active at the time of detection if the carbon dioxide concentration is 2%. In this case, worker access should be more limited, or shielding employed.

Figure 4. Left : Top and side views of the geometry in the kimberlite belt radiological exposure calculation. Right : Activity at different points (blue dot) along the side of a $20\,\mathrm{m} \times 1\,\mathrm{m}$ conveyor belt (brown dot) carrying kimberlite $10\,\mathrm{cm}$ deep.

6. Conclusion

An overview of the Mineral-PET run-of-mine diamond bearing rock sorter is presented. The paper described Monte Carlo simulation results for various aspects of the activation and detection stages. Minimum Detection Limits for the diamond size in a realistic plant were identified. The most recent results for the calculation of the residual activity of the irradiated kimberlite were presented. Finally, the previously developed radiological exposure modelling tools were applied to a Mineral-PET plant scenario.

References

[1] Ballestrero S, Bornman F, Cafferty L, Caveney R, Connell S, Cook M, Dalton M, Gopal H, Ives N, Lee C A, Mampe W, Phoku M, Roodt A, Sibande W, Sellschop J P F, Topkin J and Unwucholaa D A 2010 *12th International Conference on Nuclear Reaction Mechanisms* ed Cerutti F and Ferrari A (Varenna, Italy) pp 589–602
[2] Cook M 2014 *PhD Thesis : Remote Detection of Light Elements Using Positron Emission Tomography* (University of Johannesburg)
[3] Chinaka E M, van Rooyen J, Zibi Z and Connell S H 2014 *To appear in the conference proceedings of the 2012 South African Institute of Physics Conference*
[4] Cook M, Ballestrero S, Connell S and Tchonang M 2012 *To appear in the conference proceedings of the 2012 South African Institute of Physics Conference*
[5] Leo W 1994 *Techniques for Nuclear and Particle Physics Experiments: A How-to Approach* (Springer) ISBN 9783540572800 URL http://books.google.co.za/books?id=hDEbAQAAIAAJ
[6] International Atomic Energy Agency 2002 *Series No. WS-G-1.2*